Detection and Analysis of Surface Shape Deviation of Knee Prosthesis and Mechanical Arm Polishing Method

Bin Zhu, Shuai Wang, MingYi Zhang

***Abstract*—The research and development in the field of robotic arm industry has brought opportunities for the industrial manufacturing of medical prostheses. Aiming at the difficulties and accuracy of knee joint prosthesis surface deviation polishing in traditional medicine, an improved digital detection, analysis and polishing method based on M3C2 algorithm is proposed in this paper. In this method, 3D scanning technology is used to measure prostheses, complete 3D point cloud data is obtained, and the obtained standard and non-standard model point clouds are preprocessed. The two point clouds were registered by the double registration module of Maximal cliques and ICP algorithm. The improved M3C2 algorithm combined with the local similarity algorithm was used to compare the point clouds and detect the error, and the shape error, error distance and direction of the surface points of the knee joint prosthesis were quantified. Experimental results show that the method is effective and feasible. The method proposed in this paper can effectively extract the quantified error location, error distance and direction, which provides a feasible scheme for the automatic grinding and polishing of knee prosthesis by robotic arm, and an effective simulation experiment is carried out.**

***Index Terms*—knee prosthesis, digitization, deviation detection, error localization**

I. Introduction

The aging of the world population is increasing, and more and more elderly patients choose to take artificial knee prosthesis replacement surgery to treat joint diseases and restore the normal function of the joint.Artificial knee prosthesis replacement surgery is to replace the worn or diseased knee joint in the human body through surgery, so as to relieve pain, obtain long-term stable normal function, and restore human health. With the increase of disease population, the use of knee prosthesis consumables is also increasing.Knee prostheses are mostly made of alloy materials, of which the femur side is generally made of cobalt-chrome-molybdenum alloy, and the tibia side is generally made of titanium alloy. Knee prostheses need to be implanted into the human body and ensure long-term normal work, so the surface treatment is extremely important.At present, knee prosthesis is still mainly used by manual grinding and polishing technology. The pain points of manual grinding are very obvious:(1) High labor cost; (2) Low work efficiency, polishing efficiency is susceptible to worker factors; (3) There is a deviation in the precision of the joint, that is, the accuracy is low, and the accuracy and tolerance depend on the experience of the workers;(4) The working environment of workers is harsh, and the harmful dust in the polishing process threatens the life and health of workers.Artificial polishing cannot be mass-produced for prostheses to meet surgical needs. Therefore, it is urgent to solve the problem of digitization and automation in the process of prosthesis polishing.

Manuscript received February 08, 2025

Bin Zhu, School of Software, Tiangong university, Tianjin ,China.
Shuai Wang, School of computer science and technology, Tiangong university, Tianjin ,China.
MingYi Zhang, School of computer science and technology, Tiangong university, Tianjin ,China.

II. Related Works

The research and development in the field of industrial robot arm and digital inspection provide a certain possibility for the automatic grinding and polishing of knee prosthesis. In this field, there have been some researches on grinding and polishing methods based on digital detection technology. Liang et al [2] proposed an integrated robot polishing trajectory planning method using point cloud processing technology. In this method, the measured point cloud is preprocessed by filtering and plane segmentation, then the blade point cloud is extracted, and the initial point set is created by point cloud slicing and intersection method. Finally, Douglas-Peucker algorithm and pose frame estimation were used to extract the cutter position and optimize the contact attitude. The experimental results show that this method greatly reduces the roughness of the surface coating and makes the surface smooth. Feng et al [3] proposed a feature-guided trajectory generation method based on point cloud data, which can efficiently process welds. In this method, 3D scanning is used to measure the point cloud data of the workpiece, moving average filter is used to fit the parent curve of each scan line, and weld features are extracted from the scattered point cloud through feature recognition. Finally, the path and attitude of the robot are calculated. Compared with the reverse engineering method, the algorithm quantifies the maximum RMS error more accurately and the processing time is faster. Kuss et al [4] proposed to deduce the possible changes of the geometric model by using the dimensional tolerance of parts, match each predicted point cloud with the actual measured point cloud by ICP algorithm, calculate the point distance for shape similarity assessment, and then determine the similar geometric model for trajectory planning and workpiece positioning.

In the existing research, the registration algorithms of point cloud have developed rapidly, and there are a large number of fast and accurate registration algorithms, but there is a lack of direct defect comparison algorithms after registration. At the

same time, the quantitative extraction of the shape error, error distance and direction of the non-standard workpiece point cloud and the standard workpiece point cloud is lacking, and the point cloud comparison results cannot be directly applied to the grinding work of the robot arm. With the increasing demand of knee prosthesis, the problems of digitization and automation in the process of prosthesis polishing are becoming more and more serious. Therefore, an improved digital inspection analysis and grinding method based on M3C2 algorithm is proposed in this paper, and the digital inspection analysis and grinding process is applied to the field of joint prosthesis grinding for the first time.The method collected the standard workpiece point cloud and the non-standard workpiece point cloud, used the double registration module of the Maximal cliques and ICP algorithm to register the point cloud, used the M3C2 algorithm improved by local similarity for comparison and error detection, quantified the shape error, error distance and direction of the surface points of the knee prosthesis, and transmitted the obtained results to the simulation robot arm. It provides a feasible solution for error quantification and automatic grinding and polishing of knee prosthesis.

III. METHOD

The method focuses on detecting the surface region shape deviation between the standard point cloud and the non-standard point cloud model, and transmits the quantized results to the robot arm for simulation route simulation. The overall flow of this method is shown in Figure 1.

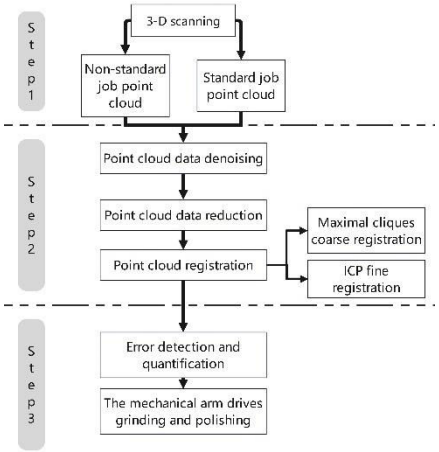

Fig.1 Overview flow chart

A. Point cloud acquisition

Three-dimensional scanning technology is used to collect and extract the workpiece point cloud. A 3D point cloud scanning system is built by rotating platform, 3D scanner and computer, as shown in Figure 2.

Fig.2 3D point cloud scanning system

The 3D scanner is used as the acquisition sensor to scan and obtain the workpiece point cloud data. In the acquisition process, the rotating platform is rotated at 2 degrees as an interval to obtain the high-precision scanning point cloud. When scanning, the scanning workpiece is placed in the center of the rotating platform, and the rotating platform is rotated at intervals to scan the standard workpiece and non-standard workpiece respectively, and the scanner can scan the workpiece point cloud completely. The computer uses NVIDIA GTX1060 graphics card and Intel i7-8750H platform, and the computer configuration can meet the requirements of point cloud data acquisition.

B. Point cloud data denoising

The scanner can scan the point cloud data within the measurement range. Due to the wide scanning range, the scanning point cloud will contain some redundant anomalies caused by scene noise and workpiece reflection, so it is necessary to de-noise the point cloud data to avoid affecting the subsequent segmentation and processing.

In this method, a statistical filter is used to denoise the point cloud and remove the scene noise and redundant outliers. The statistical filter can better remove the outlier noise, while retaining the shape characteristics of the point cloud, and will not cause too much change to the shape of the point cloud, so as to ensure that the subsequent processing steps can be accurate. The principle of statistical filter is as follows: Calculate the average distance between a point in the point cloud and its nearest n neighbor points, and then the points that do not meet the standard average distance are regarded as outliers, and the outliers can be removed.

First, the distance between each point and its nearest n neighbors is calculated, and the average value is taken, which forms a Gaussian distribution.

$$\mathrm{d_i} = \sqrt{(x_i - x_{i'})^2 + (y_i - y_{i'})^2 + (z_i - z_{i'})^2} \quad (1)$$

$$\bar{\mathrm{d}}_i = \frac{1}{n}\sum_{i=1}^{n} d_i \quad (2)$$

Then calculate the mean distance and standard deviation of all points in the point cloud.

$$\delta = \frac{1}{\mathrm{N}}\sum_{i=1}^{N} d_i \quad (3)$$

$$\sigma = \sqrt{\frac{1}{N}\sum_{i=1}^{N}(d_i - \delta)^2} \quad (4)$$

Then calculate the standard mean distance $l = \delta + \lambda \cdot \sigma$, where λ is the calculation factor. When the average distance of a point is greater than l, the point is marked as an outlier and removed. Traversing all points in the point cloud completes the statistical filtering of the point cloud.

The point cloud after denoising and statistical filtering is shown in Fig.3. After statistical filtering, outliers are effectively removed.

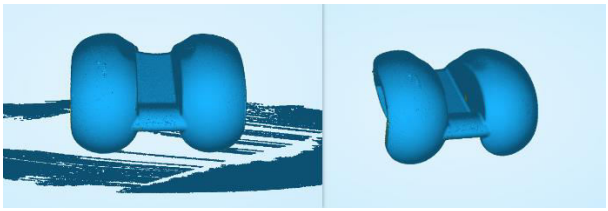

Fig.3 Unfiltered images and filtered images

C. Point cloud data reduction

In this method, point cloud curvature downsampling is used to simplify point cloud data. Due to the particularity of the workpiece surface, it needs to retain most of the surface geometric feature information, and curvature downsampling can obtain more sampling points where the point cloud curvature is larger. The principle of sampling under curvature is as follows: Firstly, the curvature search radius and point cloud nearest neighbor k are determined, and the KDTree of point cloud is constructed. The algorithm then uses KDTree and the specified search radius and nearest neighbor k search to find nearest neighbor points within the specified radius. Then calculate the Angle value of the normal from the point to the nearest neighbor, so as to approximate the effect of calculating the curvature, and can obviously improve the calculation efficiency. Set an Angle threshold. If the included Angle value is greater than the set threshold, it is considered as an area with obvious features; if the included Angle value is less than the set threshold, it is considered as an area with no obvious features. At the same time, the two types of regions are uniformly sampled, and the sampling number is $N\cdot(1-J)$ and $N\cdot J$, where N is the target sampling number and J is uniform sampling.

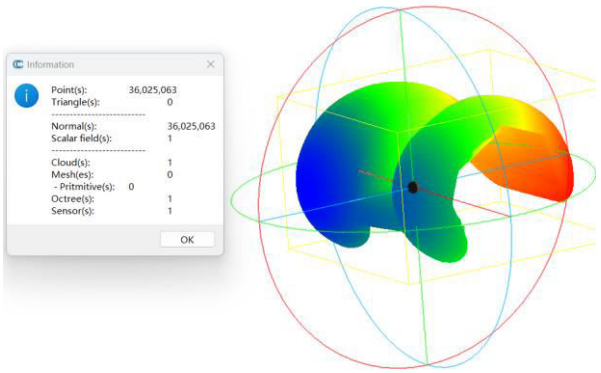

Fig.4 Pre-sampling results

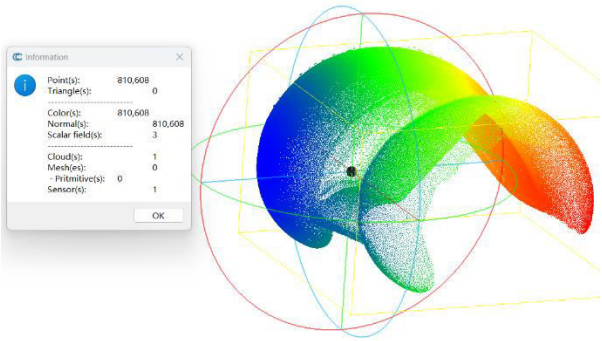

Fig.5 post-sampling results

D. Point cloud registration

In this paper, a dual registration module based on Maximal Cliques (MAC) and ICP algorithm is proposed for point cloud registration. In the module, the Maximal Cliques algorithm is first used for rough registration of point clouds, and the point clouds after rough registration have similar positions. Then ICP algorithm is used for fine registration of point clouds to achieve accurate registration results. In the module, the maximum cluster algorithm is first used for rough registration of point clouds, and the point clouds after rough registration have similar positions. Then ICP algorithm is used for fine registration of point clouds to achieve accurate registration results.

First, the Maximal Cliques algorithm is used for rough registration of the point cloud to find the close registration location. The process is shown in the figure:

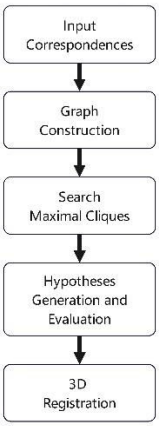

Fig.6 flow chart

For the two point clouds to be registered, assumed to be ρ_s and ρ_{us} , the local features are extracted using geometric descriptors, and the initial corresponding point set is formed from the matched feature descriptors. The compatibility graph is then constructed from an initial set of corresponding points, where the correspondence represents geometrically compatible nodes and the edges connecting nodes. The first order graph (FOG) is constructed by rigid distance constraints between pairs of responses (p_i, p_j) .The first order graph can be represented as follows:

$$L_{dist}(p_i, p_j) = \left\| p_i^{\,s} - p_j^{\,s} \right\| - \left\| p_i^{\,us} - p_j^{\,us} \right\| \quad (5)$$

The compatibility score between p_i and p_j is given by the formula:

$$L_{cs}(p_i, p_j) = \exp\left(-\frac{L_{dist}(p_i, p_j)^2}{2d_{cs}^{\,2}}\right) \quad (6)$$

Where d_{cs} is the distance parameter. Where, if $L_{cs}(p_i, p_j)$ is greater than the given threshold ϕ , then p_i and p_j form a side γ_{ij} , and $L_{cs}(p_i, p_j)$ is the weight of γ_{ij} , otherwise $L_{cs}(p_i, p_j)$ is set to 0. Since the consistent graph is undirected, the weight matrix W_{FOG} is symmetric.

Construct a second-order graph using the following formula:

$$W_{SOG} = W_{FOG} \bullet (W_{FOG} \times W_{FOG}) \quad (7)$$

Where $\bullet$ represents the element-wise product between

two matrices.

In a given undirected graph, a clique is its complete subgraph, and a maximal clique is a clique that is not contained by any other clique. After constructing the second-order graph, we search the maximal clique in the graph and get the maximal clique set MAC_{init}. Because of the large number of groups found in the maximal group set, it is necessary to introduce a group reduction algorithm to filter out some useless groups. First calculate the weight of each clique in the maximal clique, given the clique $C_i = (V_i, E_i)$, where V represents an edge and E represents a vertex. The weights are calculated using a formula:

$$\omega_{C_i} = \sum_{e_j \in E_i} \omega_{e_j} \tag{8}$$

Where ω_{e_j} represents the weight of e_j in the middle of W_{SOG}. Since multiple maximal cliques may contain a specific node at the same time, only the maximal clique with the highest weight is chosen as the unique maximal clique of the node. Then we sort by the weight of the clique, taking the first k bits in the sorting sequence as the likely correct hypothesis.

Each maximal clique after filtering represents a set of correspondence, and the pose hypothesis of 6 degrees of freedom can be calculated by applying SVD algorithm to each set of correspondence. The weight SVD method is adopted here. Here we calculate the principal eigenvalue of W_{SOG} as the corresponding weight.

The goal of point cloud registration is to estimate the optimal rigid body transformation matrix by estimating the maximum objective function:

$$(\Re^*, t^*) = \arg\max_{\Re, t} \sum_{i=1}^{N} s(p_i) \tag{9}$$

Where $p_i \in P_{initial}$ (initial correspondence set), $N = |P_{initial}|$, $s(p_i)$ indicates the score of p_i. After calculation, the coarse registration matrix of point cloud is obtained, and then ICP algorithm is used to perform fine registration of point cloud to obtain the final registration matrix.

Fig.7 Final alignment matrix

E. Error detection and processing

Thanks to the rapid development of ground-based laser scanners (TLS), more and more measurement techniques are being used to track the evolution of three-dimensional natural surfaces with previously unmatched resolution and precision. At the same time, there are relatively few solutions for 3D point cloud correlation, and it is difficult to accurately compare complex natural surfaces, which creates a huge obstacle in the field of geosurveying. Therefore, the M3C2 algorithm is proposed to directly compare the surface differences of point clouds and track the three-dimensional changes of surface direction. However, due to the calculation process of M3C2 algorithm, M3C2 algorithm can not directly calculate the direct normal distance between the corresponding points, nor can it be directly applied to the error quantization and mechanical arm grinding. Therefore, local similarity algorithm is used to improve M3C2 algorithm to calculate the exact distance between point pairs.

Three-dimensional surface normal calculation. First of all, we have carried out curvature downsampling on the point cloud in the point cloud preprocessing stage, and the point cloud after downsampling is taken as the core point of calculation. For any point, the normal of the point is calculated, and the normal vector and direction of each point are defined by fitting the polynomial surface or plane to the neighborhood NN_i of the point.

Distance calculation between point clouds. After defining the normals at each point, the point i is projected along the normals to another point cloud with a radius d. The projection is made by constructing a cylinder of radius d with the central axis of the cylinder passing through point i and along the normal direction. Two subsets can be selected by the projection cylinder, which are the standard workpiece point set and the non-standard workpiece point cloud. The local similarity algorithm is used to calculate the similarity and distance of the two corresponding point sets. Reciprocal weighted modulus (RWME) is used here to evaluate the partial similarity between two three-dimensional objects, that is, the partial similarity is defined as the ratio of the weighted surface area of the model to the weighted unilateral Hausdorff distance from the model to the point cloud. Define the RWME between p_s and p_{us} point clouds as:

$$R(X,Y) = \frac{\sum_{i=1}^{N} \omega_i |X_i|}{\lambda + \sum_{i=1}^{N} \omega_i d(X_i, Y)} \tag{10}$$

Where λ is a positive number, which is fixed as 0.43 in this experiment, and ω_i is the weight.

Here ω_i uses smooth RWME, ω_i is defined as:

$$\omega_i = \exp\left(\frac{-d(X_i, Y)}{h}\right) \tag{11}$$

$$d(X,Y) = \max_{x \in X} d(x,Y) \tag{12}$$

Formula 12 is the one-way Hausdorff distance from A to B (OHD).

$$d(x,Y) = \min_{y \in Y} \|x - y\| \tag{13}$$

The local similarity parameters of two subsets of point clouds can be calculated from the above formula, where the larger the RWME, the more similar the local area is. According to the local similarity combined with the point cloud cylinder radius, the cylinder radius is adjusted by RWME. The larger the RWME, the more similar the local point cloud is, and the radius can be enlarged to ensure the calculation speed without misalignment; the smaller the RWME, the less similar the local point cloud is, and the radius is reduced. After adjusting the radius, the optimal solution is selected, and the nearest point pair of normal in the two-point cloud is matched, and the point pair distance is calculated after matching.

After calculating the entire point cloud, the error point, error distance and error direction can be obtained, and then the data can be exported.

Fig.8 Selected outcome data

F. *Mechanical arm drive grinding and polishing*

In this paper, the DOFBOT robot arm of Yahboom is used for experiments. The simulation system was written by ROS and adopted Moveit! Simulation of grinding data and path. In the simulation system, the device location and device size are the same as in the real environment, and the workpiece model is generated by the scan point cloud. The simulation system calculates the trajectory of the detected error points, and then interpolates the calculated segmented trajectory, or splits or splices different trajectories to generate a complete grinding trajectory.

IV. Experimental Results

In order to verify the validity of this paper, we collected existing standard and non-standard workpieces, and conducted experiments on the proposed algorithm. By comparing the algorithms, quantified error fix points, error distance and direction can be completely extracted, and can be transmitted to the robot arm for path planning and polishing. Comparing the M3C2 algorithm plug-in in CloudCompare with the M3C2 algorithm proposed in this paper, the results show that the M3C2 algorithm in CloudCompare cannot extract the error region information and cannot be used for subsequent robotic arm grinding. Meanwhile, the improved M3C2 algorithm proposed in this paper is more parametric. It can extract more abundant and accurate error information by itself.

In addition, the algorithm proposed in this paper obtains relatively more delicate and accurate results, indicating that the algorithm has better error detection and extraction capabilities, and can meet the practical needs to a certain extent.

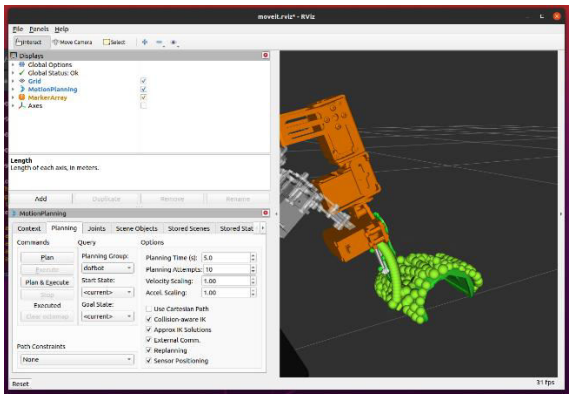

Fig.9 Grinding Schematic

V. Conclusion

In this paper, an improved digital detection, analysis and grinding method based on M3C2 algorithm is proposed to solve the problems of insufficient precision and labor cost in the automatic grinding and polishing of knee prostheses. This algorithm combines the local similarity and M3C2 algorithm to refine the error detection granularity to the local region, and introduces M3C2 algorithm into the field of industrial error detection and grinding for the first time, which can extract the error information better. The experimental results show that the proposed algorithm can completely extract and quantify the workpiece error, and complete the path planning of the grinding trajectory with the robot arm, which can better realize the digital grinding and polishing of joint prosthesis. The digital grinding and polishing of joint prosthesis has a good research prospect and can promote the development of medical prosthesis processing and digitization to a certain extent.

References

[1] G. O. Young, "Synthetic structure of industrial plastics (Book style with paper title and editor)," in *Plastics*, 2nd ed. vol. 3, J. Peters, Ed. New York: McGraw-Hill, 1964, pp. 15–64.

[2] W.-K. Chen, *Linear Networks and Systems* (Book style). Belmont, CA: Wadsworth, 1993, pp. 123–135.

[3] H. Poor, *An Introduction to Signal Detection and Estimation*. New York: Springer-Verlag, 1985, ch. 4.

[4] B. Smith, "An approach to graphs of linear forms (Unpublished work style)," unpublished.

[5] E. H. Miller, "A note on reflector arrays (Periodical style—Accepted for publication)," *IEEE Trans. Antennas Propagate.*, to be published.

[6] J. Wang, "Fundamentals of erbium-doped fiber amplifiers arrays (Periodical style—Submitted for publication)," *IEEE J. Quantum Electron.*, submitted for publication.

[7] C. J. Kaufman, Rocky Mountain Research Lab., Boulder, CO, private communication, May 1995.

[8] Y. Yorozu, M. Hirano, K. Oka, and Y. Tagawa, "Electron spectroscopy studies on magneto-optical media and plastic substrate interfaces(Translation Journals style)," *IEEE Transl. J. Magn.Jpn.*, vol. 2, Aug. 1987, pp. 740–741 [*Dig. 9th Annu. Conf. Magnetics* Japan, 1982, p. 301].

[9] M. Young, *The Technical Writers Handbook.* Mill Valley, CA: University Science, 1989.

[10] (Basic Book/Monograph Online Sources) J. K. Author. (year, month, day). *Title* (edition) [Type of medium]. Volume(issue). Available: http://www.(URL)

[11] J. Jones. (1991, May 10). Networks (2nd ed.) [Online]. Available: http://www.atm.com

[12] (Journal Online Sources style) K. Author. (year, month). Title. *Journal* [Type of medium]. Volume(issue), paging if given. Available: http://www.(URL)

[13] R. J. Vidmar. (1992, August). On the use of atmospheric plasmas as electromagnetic reflectors. *IEEE Trans. Plasma Sci.* [Online]. *21(3).* pp. 876—880. Available: http://www.halcyon.com/pub/journals/21ps03-vidmar